Available online at www.sciencedirect.com
ScienceDirect
Applied Catalysis A: General 328 (2007) 226–236
APPLIED CATALYSIS A: GENERAL
www.elsevier.com/locate/apcata

New green catalytic manufacture of glutaric acid from the oxidation of cyclopentane-1,2-diol with aqueous hydrogen peroxide

Hui Chen [a], Wei-Lin Dai [a,*], Ruihua Gao [a], Yong Cao [a], Hexing Li [b], Kangnian Fan [a]

[a] *Department of Chemistry and Shanghai Key Laboratory of Molecular Catalysis and Innovative Materials, Fudan University, Shanghai 200433, PR China*
[b] *Department of Chemistry, Shanghai Normal University, Shanghai 200234, PR China*

Received 20 November 2006; received in revised form 4 June 2007; accepted 15 June 2007
Available online 23 June 2007

Abstract

Selective oxidation of cyclopentane-1,2-diol to glutaric acid (GAC) over different kinds of materials has been carried out with aqueous hydrogen peroxide. The homogenous tungstic acid catalyst was tried first, which showed a yield of GAC as high as 91.2%. However, the separation, recovering and reusing of the homogeneous catalyst are very difficult, thus restricting its further application in industry. Then tungsten-containing mesoporous silica (W-MCM-41) was next tried as a heterogeneous catalyst. Although the activity was about 20% lower than that of the homogeneous one, it was much more easily to be separated, recovered and reused. It is interesting to find that the phase-transfer material shows the best performance in the reaction, during which the yields of GAC on $[\pi\text{-}C_5H_5NC_{16}H_{33}]_2\{W_2O_3[O_2]_4\}$ (CW) and $[\pi\text{-}C_5H_5NC_{16}H_{33}]_3\{PO_4[WO_3]_4\}$ (CPW) were 91.3 and 94.3%, respectively. These two materials demonstrated the characteristic features of ''reaction-controlled phase-transfer''; the samples dissolved during the reaction and precipitated after the reaction. Therefore, these materials show the advantages of both homogeneous and heterogeneous catalysis and can easily be recovered and reused. The fresh samples and the recovered ones were all characterized by FT-IR, Raman, ^{31}P NMR and XPS spectroscopy. The structures of these two materials all changed after the reaction, polymerizing by forming W–O_c–W (edge-sharing) bonds. XPS results revealed that the recovered samples of CW and CPW are all more stable than the corresponding fresh ones due to the changes of the coordination circumstances.

Keywords: Cyclopentane-1,2-diol; Glutaric acid; Selective oxidation; Hydrogen peroxide; Homogeneous catalyst; Heterogeneous catalyst; Phase-transfer catalyst

1. Introduction

Dicarboxylic acids, including glutaric acid (GAC), adipic acid, trimethyladipic acid, and dodecanedioic acid, are essential feed-stocks for the manufacture of polyamides, polyesters, plasticizers, and lubricating oils [1]. The anhydrides, one of the monomers of LCD materials, can also be synthesized from dicarboxylic acids; however, there is no convenient method for the production of GAC yet, especially on a large-scale for industry. The current manufacture process is in multi-steps by oxidative cleavage of C–C bonds of mixtures containing the corresponding cyclic alcohols and ketones and their derivatives with nitric acid [2–4]. Noyori and co-workers [5,6] have developed a general method of synthesizing carboxylic acids, including adipic acid and GAC, in which Na_2WO_4 and $[CH_3(n\text{-}C_8H_{17})_3N]HSO_4$ were used as the oxidation and phase-transfer catalysts, respectively. The latter is quite expensive and cannot be easily separated and recovered. Thus, this process is impossible for large-scale industrial production of GAC.

In our previous work, a novel green process of synthesizing GAC from cyclopentene (CPE) with high GAC yield of 92.3% has been developed without using any kinds of solvents; in this process only 50% aqueous H_2O_2 solution and tungstic acid were used as the oxidant and the catalyst, respectively [7]. We also succeeded in the using of a phase-transfer material in synthesizing GAC from CPE; the yield is also very high (83.1%) [8]. However, the boiling point of CPE is 319 K, so it can easily evaporate and escape from the plant, thus resulting in the inevitable loss when in use and in great difficulties in its storage and transportation. Hence, the CPE process is inconvenient and not economic. Therefore, some other alternative derivatives from CPE can be chosen. It is found

* Corresponding author. Tel.: +86 21 55664678; fax: +86 21 65642978.
E-mail address: wldai@fudan.edu.cn (W.-L. Dai).

0926-860X/$ – see front matter © 2007 Elsevier B.V. All rights reserved.
doi:10.1016/j.apcata.2007.06.021

that cyclopentane-1,2-diol (CPDL), which can be easily obtained quantitatively from CPE with aqueous hydrogen peroxide, can be selected as a good substitute of CPE because of its high boiling-point as well as its excellent ability to mix with water when handed with aqueous hydrogen peroxide. In addition, CPDL is the main by-product in the process of glutaraldehyde from the selective oxidation of CPE, as reported in our previous work [10]. So the present process can be a good supplement for the previous glutaraldehyde process, thus making the whole process much economic and perfect, considering its abundant products and zero draining. In this research, three kinds of materials were tried in the novel process (homogeneous tungstic acid, heterogeneous WO_3/SiO_2 catalyst and tungsten-containing phase-transfer material). The recovering and reusing conditions of the heterogeneous and phase-transfer materials were also investigated. The fresh and recovered phase-transfer materials were all characterized by FT-IR, Raman, ^{31}P NMR and XPS spectroscopy to reveal the structure changes after the reaction.

2. Experimental

2.1. Preparation

2.1.1. Preparation of W-MCM-41

W-MCM-41 was synthesized via an in situ method according to the literature [9]. 12.4 g of cetylpridine bromide ($CPBR{\cdot}H_2O$) was added to 120 mL of HCl (5 M) to give a mixture. Next 22.4 mL of tetraethyl orthosilicate (TEOS) and different amounts of aqueous sodium tungstate solution ($Na_2WO_4{\cdot}2H_2O$, $2H_2O$, 0.2 M) were simultaneously and quickly added into the mixture under vigorously stirring to give a pale-yellow gel. After vigorous stirring for 1 h, the gel was aged at 323 K under moderate stirring for 24 h, and then filtered and washed with distilled water. The precipitate was dried at 393 K and calcined at 873 K in air to obtain the W-MCM-41. The pure silica MCM-41 was synthesized by omitting the adding of $Na_2WO_4{\cdot}2H_2O$. For the purposes of comparison, the WO_3-supported catalysts were prepared through the conventional incipient wetness impregnation method as follows: 0.23 g of ammonium tungstate ($(NH_4)_5H_5[H_2(WO_4)_6]{\cdot}H_2O$) was dissolved in a solution of ammonium. Into the stirred solution was dispersed 1 g of pure MCM-41 at 323 K. After the water evaporated completely, the dried solid was further calcined at 873 K in air for 4 h to obtain the WO_3/MCM-41. W-SBA-15 were also synthesized for comparison, according to the literature [10].

2.1.2. Preparation of the phase-transfer material

The phase-transfer material $[\pi\text{-}C_5H_5NC_{16}H_{33}]_3\{PO_4[WO_3]_4\}$ was prepared according to the procedure described previously [11,12]. A suspension of tungstic acid 2.5 g (10 mmol) in 7 mL of aqueous H_2O_2 (35%) was stirred and heated to 333 K until a colorless solution was obtained. The solution was filtered and then cooled to room temperature. After that, 40% (w/v) H_3PO_4 (0.62 mL, 2.5 mmol) was added to the solution, which was then diluted to 30 mL with distilled water. An amount equal to 1.80 g of cetylpyridiniumammonium chloride (5 mmol) in dichloromethane (40 mL) was added dropwisely with stirring in 2 min, and the mixture was maintained for an additional 15 min. The organic phase was then separated, dried with anhydrous Na_2SO_4, filtered and evaporated under atmospheric pressure at 323–333 K (water bath). At last, about 2.5 g (85%, based on the quaternary ammonium salt charged) of the dried yellow powder was obtained by further evacuation, which was labeled as CPW.

The phase-transfer material $[\pi\text{-}C_5H_5NC_{16}H_{33}]_2\{W_2O_3[O_2]_4\}$ was prepared according to the literature [13]: 1.65 g $Na_2WO_4{\cdot}2H_2O$ (5.0 mmol) was dissolved in 10 mL of water and 6.0 mL of H_2O_2 (30%) to obtain a yellow pellucid solution. Then hydrochloric acid was titrated to the solution until a pH of 2–2.5 was obtained. An amount equal to 3.58 g of cetylpyridiniumammonium chloride (10 mmol) in ethanol (10 mL) was added dropwisely under vigorous stirring, and a white precipitate formed simultaneously. The mixture was maintained for an additional 1 h, and then filtered and washed with distilled water. After the mixture was dried completely, the material $[\pi\text{-}C_5H_5NC_{16}H_{33}]_2\{W_2O_3[O_2]_4\}$ was obtained and labeled as CW.

$[\pi\text{-}C_5H_5NC_{16}H_{33}]_7[PW_{11}O_{39}]$ (CPW11) was prepared also according to ref. [14]. Materials $[\pi\text{-}C_5H_5NC_{16}H_{33}]_3[PW_{12}O_{40}]$ (CPW12) and $[(CH_3)_3NC_{16}H_{33}]_3[PW_{12}O_{40}]$ (TPW12) were prepared according to ref. [8]. The recovered materials of CW and CPW are labeled as Re-CW and Re-CPW, respectively.

2.2. Catalytic oxidation of CPDL to GAC

A round-bottomed flask with a condensation tube was charged with the catalyst (0.1 mol WO_3), 50% H_2O_2 (19.5 mL) and CPDL (10 g). The flask was then placed in a water bath at 363 K with vigorous stirring for 8 h. After then, if necessary, the resulting suspension was centrifugated and the pellucid liquid was analyzed by titration with NaOH solution to get the yield of organic acid. The precipitated catalyst was recovered for further use.

The pellucid liquid was boiled up to bubbling to decompose the remaining peroxides (avoid explosion during vacuum distillation), until the amylum-KI test is negative. Then small amounts of activated carbon were added and the mixture was stirred in a boiling water bath for 30 min. After filtering, the colorless solution was vacuum distilled and concentrated to remove most of the water. After that, the resulting solution was refrigerated at 273 K for 24 h and colorless GAC crystals were formed. After being filtered and washed with small amounts of ice water, the as-obtained crystals were dried at 363 K for 12 h for the future analysis. The filtrate can be further dehydrated to get more GAC crystals that can be mixed with those from the first step for the accurate analysis of pure GAC yield. The yield of GAC was determined with acid-base titration, while the purity of GAC was analyzed with melting point test, HPLC and GC (after esterification with methanol).

2.3. Characterization

The high-angle X-ray powder diffraction (H-XRD) patterns were recorded on a Bruker D8 Advance spectrometer with Cu

Kα radiation, which was operated at 40 mA and 40 kV. The specific surface areas, the pore volumes and the mean pore diameters of the samples were measured with a Micromeritics Tristar BET spectrometer by using liquid nitrogen at 77 K and calculated according to the BET method. The tungsten contents in W-MCM-41 and W-SBA-15 were determined by the inductively coupled argon plasma method (ICP, IRIS Intrepid, Thermo Elemental Company) after solubilization of the samples in HF:HCl solutions.

The laser Raman experiment were performed by using a Jobin Yvon Dilor Labram I Raman spectrometer equipped with a holographic notch filter, a CCD detector and a He–Ne laser radiating at 632.8 nm. The FT-IR measurements were carried out with a Nicolet Model 205 spectrometer, using KBr pellet technique. ^{31}P NMR spectra of solid samples were collected in a Brucker DXR 400 spectrometer. XPS experiments were carried out with a Perkin-Elmer PHI 5000 C ESCA system using Al Kα radiation (1486.6 eV) at a power of 250 W. The pass energy was set as 93.9 eV and the binding energies were calibrated by using contaminant carbon at BE of 284.6 eV.

3. Results and discussion

3.1. Homogeneous catalysis

Homogeneous catalyst is the most common and classical catalyst in the aqueous oxidation reactions, because it can be dissolved in the reaction system and shows very high activity and efficiency. Typical homogeneous tungstic acid (H_2WO_4) catalysts were used in the oxidation of CPE with aqueous H_2O_2 in our previous work [7], and the yield of GAC can reach 92.3%. This is a novel green process for the manufacture of GAC because no organic solvents were used, and no additive except H_2O_2 was added. Hence, the only by-product is water, and no pollutants are produced. However, it is not convenient to use CPE as the raw material because of its low boiling point, as mentioned in the Section 1. To the best of our knowledge, no reports have been published about the manufacture of GAC from the catalytic oxidation of CPDL. Since CPDL is an important intermediate in the process of GAC from CPE, we can easily choose tungstic acid as a homogeneous catalyst in the new green process of GAC from CPDL. Detailed reaction results are shown in Table 1.

The reaction temperature plays a great role on the yield of GAC. The yield of GAC increases as the temperature increases until the reaction temperature reaches 353 K because a high reaction temperature is needed to supply adequate energy for the cleavage of C–C bonds. However, further increase of the temperature leads to a decrease of a GAC yield, which can be easily interpreted as due to the formation of some byproducts and deep oxidation occurrence with the further high temperature. The reaction time is also one of the important reaction parameters that should be controlled properly. In general, 5 h is enough for the title reaction and further prolonging the reaction time cannot increase the GAC yield much. Under an optimal reaction condition, the yield of GAC can reach 91.2%. It is found that all the hydrogen peroxide was consumed and the efficiency of hydrogen peroxide is also very high (see Table 1). After the reaction, $PbCO_3$ (molar ratio of $PbCO_3$ to H_2WO_4 is 1:1) was added to make H_2WO_4 precipitate as $PbWO_4$. After the mixture was boiled at 373 K for 2 h, the suspension was filtered and the tungsten oxide in the separated solid mixture can be recovered by treatment with strong hydrochloric acid and reused in the next entry. The pellucid solution was further treated as mentioned in section 2.2, so that pure GAC crystals can be obtained. The purity of the resulting GAC solid is over 99% (analyzed by GC) and the melting point is 369–370 K, similar to the literature value of 370–371 K. Therefore the resulting GAC product synthesized in this process is pure enough to be used directly in most fields without any further purification.

Table 1
Selective oxidation of CPDL to GAC over the homogeneous tungstic acid catalyst

Reaction temperature (K)	Reaction time (h)	Yield of GAC (%)	Efficiency of H_2O_2 (%)
333	5	41.2	37.5
343	5	67.2	61.1
353	5	91.2	82.9
358	5	85.9	78.1
363	5	84.5	76.8
353	4	89.7	81.5
353	6	91.2	82.9
353	7	91.9	83.5

Reaction conditions: CPDL (1 g); catalyst:H_2O_2:CPDL = 0.02:3.3:1 (molar ratio); the yield of GAC was based on CPDL.

Though the homogeneous catalyst H_2WO_4 is efficient, and can be recovered and reused, the post-treatment is too complicated and the high content of tungsten contaminant in the final product mixture makes this process very inconvenient because it requires further purification. Therefore, the problem diverts to the finding of new catalyst that is easy to be recovered and reused. It is natural to find that a heterogeneous catalyst is preferred.

3.2. Heterogeneous catalysis

Heterogeneous catalysts are also widely used in most liquid phase reactions, especially as the mesoporous materials with

Table 2
Catalytic performance in the selective oxidation of CPDL to GAC over various heterogeneous catalysts

Catalyst	$C_{H_2O_2}$ (wt.%)	Yield of GAC (%)	Efficiency of H_2O_2 (%)
10% W-MCM-41	50	60.2	45.2
20% W-MCM-41	50	70.5	52.9
30% W-MCM-41	50	54.3	40.7
20% WO_3/MCM-41	50	66.3	49.7
20% W-SBA-15	50	58.6	44.0
20% WO_3/MCM-41	30	54.3	40.7

Reaction conditions: CPDL (1 g); catalyst:H_2O_2:CPDL = 0.02:4.0:1 (molar ratio); reacted at 353 K for 5 h; the yield of GAC was based on CPDL.

Table 3
Physico-chemical parameters of various samples

Samples	WO_3/SiO_2[a] (wt.%)	Surface area (m^2/g)	Pore volume (cm^3/g)	Pore diameter (nm)
MCM-41	0	1218	0.63	2.6
W-MCM-41 (10%)	10	945	0.42	2.9
W-MCM-41 (20%)	20	944	0.51	2.9
W-MCM-41 (30%)	30	792	0.49	2.9
WO_3/MCM-41 (20%)	20	414	0.49	4.8
W-SBA-15 (20%)	20	571	1.1	4.3

[a] Stoichiometric ratio in gel.

the active species doped on. Such popularity reflects the findings that these materials have unique advantages: (1) their large surface areas and unique porous structure make them available for the metal or the metallic oxides to disperse well on them; (2) these insoluble solids are easy to be recovered by simple filtration or centrifugation. In our group, tungsten containing W-MCM-41 and W-SBA-15 were successfully synthesized via an in situ method [9,10], they all present high activity in the selective oxidation of CPE to glutaraldehyde with H_2O_2. Hence we tried these catalysts with different tungsten loading values in the oxidation of CPDL to GAC by aqueous H_2O_2.

3.2.1. Catalytic activity test

The results of the selective oxidation of CPDL to GAC (GAC) over several W-containing heterogeneous catalysts are listed in Table 2. We found that the GAC yields over these heterogeneous catalysts are much lower than that of the homogeneous one, at least 21% lower. And more H_2O_2 was needed because the mesoporous materials would cause part of the H_2O_2 to decompose during the reaction. So the efficiency of H_2O_2 is also very low. However, the heterogeneous catalysts are convenient to be recovered and reused, thus making them a kind of important alternative in special cases. From Table 2 we can see that the GAC yield is strongly dependent on the content of the tungsten in the W-containing MCM-41 samples, which reveals that the optimum catalyst in the present reaction is the one with 20% WO_3 content. The method of synthesizing the catalysts also has a great influence on their activity. The GAC yield over the supported WO_3/MCM-41 is lower than the corresponding W-doped-MCM-41, with the same WO_3 content of 20%. The activity of W-SBA-15 is also lower than that of the W-MCM-41 catalyst, indicating that the property of support also influences the catalyst activity, and MCM-41 material is more proper for the present catalytic system. Some characterizations were carried out to investigate the structure effect on the activity of these catalysts.

We also investigated the effect of the concentration of hydrogen peroxide. When 30% H_2O_2 was used as the oxidant, the yield of GAC on 20% W-MCM-41 was 54.3%, 16.2% lower than the GAC yield when 50% H_2O_2 was used as oxidant. It suggests that the concentration of H_2O_2 has great effect on the reaction. High concentration of H_2O_2 leads to high reaction rate and high GAC yield. But ultra high concentration is very dangerous (>50%), so we choose 50% H_2O_2 in the present process.

3.2.2. Characterization

The physico-chemical parameters of various samples are shown in Table 3. The BET surface area and pore volume of W-MCM-41 samples are lower than the values of pure MCM-41, but the pore size is slightly higher than that of pure MCM-41, as shown in Table 3. As the WO_3 contents increase, the BET areas and pore volumes decrease abruptly, indicating the great influence of the added heteroatoms. If the amount of the added tungsten heteroatoms reaches a much higher value, the typical mesoporous structure cannot be kept. The inflection point at $P/P_0 = 0.25–0.35$ in N_2 adsorption isotherm (not shown) indicates that the W-MCM-41 samples possess regular mesopores, except for the one containing 30% WO_3, suggesting that there is no regular mesoporous structure in the 30% W-MCM-41 samples. The supported sample WO_3/MCM-41 (20%) has an extraordinarily small BET area and a large pore diameter, illustrating that most pores of MCM-41 have been blocked. Compared with W-MCM-41 sample, the W-SBA-15 material also has smaller BET area, which may be one of the reasons why the yield of GAC is lower on the 20% W-SBA-15 catalyst than on the corresponding W-MCM-41 counterpart.

The XRD patterns of various samples are shown in Fig. 1. For the 10% W-doped-MCM-41 sample, no peaks corresponding to crystalline WO_3 are observed, indicating the absence of agglomerated crystalline WO_3 in this catalyst. The result means that WO_3 is totally incorporated into the lattice of the MCM-41 structure and has a high dispersion. When the WO_3 loading exceeds 20% for the W-doped-MCM-41, characteristic peaks

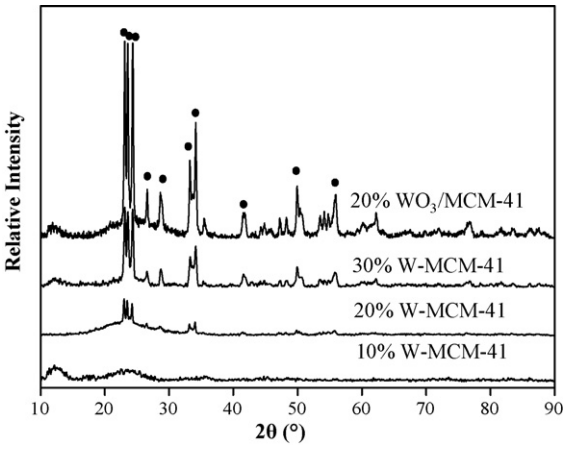

Fig. 1. XRD patterns of W-MCM-41 and WO_3/MCM-41 samples with different WO_3 contents; (●) crystalline WO_3.

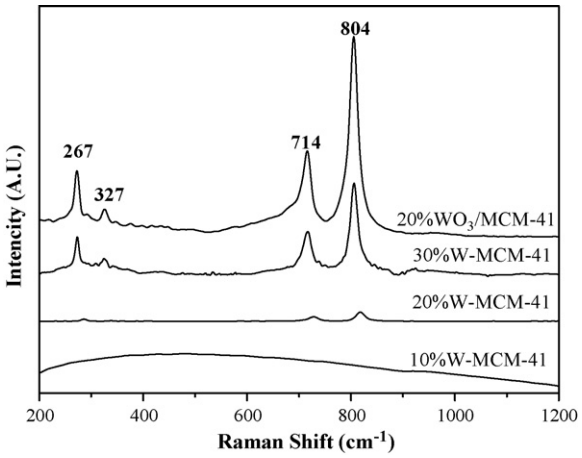

Fig. 2. Raman spectra of W-MCM-41 and WO_3/MCM-41 samples.

of crystalline WO_3 appear, suggesting that WO_3 begins to congregate. Stronger peaks can be observed for the supported WO_3/MCM-41 sample, indicating the serious congregation of WO_3 in this catalyst.

Additional information of the surface state of WO_3 species was investigated by using the confocal microprobe Laser Raman spectra, as shown in Fig. 2. No Raman bands attributed to the octahedral crystallineWO_3, e.g. at 804, 714, 327 or 267 cm^{-1}, are observed for 10% W-doped MCM-41, very similar to the case of pure MCM-41 (not shown here). For the 20% W-doped MCM-41, four weak peaks attributed to crystalline WO_3 can be observed, indicating that a small amount of WO_3 in this catalyst has begun to agglomerate and to form crystalline centers. Fig. 2 also shows the Raman spectra of samples of 30%W-doped- MCM-41 and 20% WO_3/MCM-41 supported catalyst for comparison. Obvious Raman bands ascribed to crystallineWO_3 could be detected in the figure with respect to these two samples, illustrating that the loading of excess content of tungsten species would result in the agglomeration of WO_3 on the surface. Furthermore, comparing the two catalysts: W-doped-MCM-41 and supported WO_3/MCM-41 with the same tungsten oxide loading of 20%, we can find that the latter has very strong peak intensity, even stronger than the 30% W-doped-MCM-41, while the 20% W-doped-MCM-41 presents very weak Raman bands of crystalline WO_3. That is a clear indication that the WO_3 species are well dispersed in the framework of MCM-41 material for the in situ synthesized catalysts. This finding accords well with the XRD results and with our previous work [9,10,15].

The activity results suggest the catalysts with large crystalline WO_3 are less active than the ones with high WO_3 dispersion. Agglomeration of WO_3 and the partial collapse of the mesoporous structure of the W-MCM-41 all lead to the lower GAC yields. The presence of the highly dispersed tungsten species in the silica matrix is necessary for the title reaction, which also accords well with the literature results [9,10,15].

3.2.3. The stability and leaching behavior of the catalysts

To investigate the stability and the leaching behavior of W-species into the product mixture, we detected the tungsten contents in the fresh and used W-MCM-41 catalysts by using the ICP method. For all the three samples, 50–70% WO_3-species can be kept in the heterogeneous catalysts after one reaction cycle and the used catalysts can be reused without any further treatment, making the separation of the catalyst from the reaction mixture quite easy when compared with the homogeneous catalysis process. In addition, the leached WO_3-species, which is soluble in the reaction mixture, can easily be recovered through an ion-exchange resin column. Thus, the heterogeneous process shows advantages to some extent compared with the homogeneous one, although the GAC yield is not high and some WO_3-species are still left in the products mixture.

3.3. Phase-transfer catalysis

The phase-transfer materials, especially the reaction-controlled phase-transfer materials, have attracted much research interest because of high efficiency and unique structure and solubility properties [16–23], including the selective oxidation of 1,2-diols to carboxyl acids [24]. Recently, Xi et al. [25] reported a reaction-controlled phase-transfer catalyst——$[\pi\text{-}C_5H_5NC_{16}H_{33}]_3\{PO_4[WO_3]_4\}$, which is active and selective for the epoxidation of propene with 30% H_2O_2. More interestingly, this catalyst is insoluble in both water and organic solvents, but can dissolve in organic solvents after the action of H_2O_2 and can catalyze the reaction homogeneously. After the reaction, it precipitates itself from the reaction mixture and can easily be recovered. However, the unique character of this reaction-controlled phase-transfer catalyst has not been tried in other reactions yet. We have tried to use it in the oxidation of CPE to GAC [8] and found that it has excellent activity. The yield of GAC can reach 83.1%. Considering the similarity of the reaction system, we can conclude that this material may show good catalytic performance as well as easy recovering ability in the selective oxidation of CPDL to GAC. Therefore, in the present work we tested the activity and stability of this kind of phase-transfer material. In addition, some other phase-transfer materials were also investigated to uncover the intrinsic character of the phase-transfer material.

3.3.1. Activity test

We first investigated the time course of the oxidation of cyclopentane-1,2-diol with hydrogen peroxide for the phase-transfer CPW material. As shown in Fig. 3, the reaction rate is so high that the GAC yield can reach 71.3% just after reaction for 1 h, indicating that this phase-transfer material has significantly high activity. As the time went on, the GAC yield increased. After 5 h, the GAC yield reaches the maximum value. Further prolonging the reaction time cannot increase the GAC yield, so 5 h is enough for this reaction system.

Several phase-transfer materials with different quaternary ammonium cations and different polyoxometalate (POM) anions were tried in the selective oxidation of CPDL as well as other substrates (olefin, 1,2-diol, ketone) to the corresponding dicarboxylic acids by using aqueous H_2O_2. As shown in Table 4, for the five samples, only CW and CPW showed the

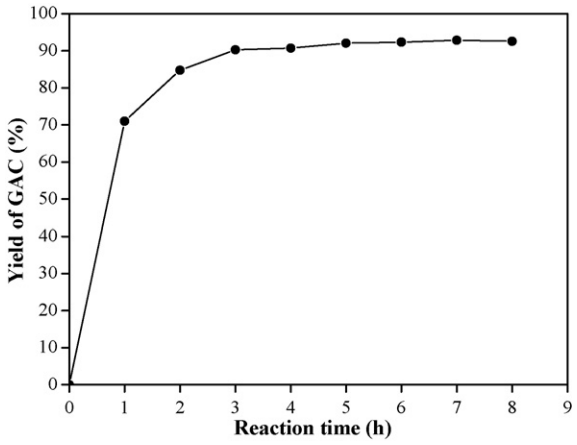

Fig. 3. Time course of the oxidation of cyclopentane-1,2-diol with hydrogen peroxide for the CPW catalyst. Reaction conditions: $n_{substrate}$:$n_{H_2O_2}$:$n_{cat.(W)}$ = 1:3.3:0.02; reaction temperature: 363 K.

reaction-controlled phase-transfer character. They dissolved completely during the reaction and pellucid solutions were obtained. After the reaction had been performed at 363 K for 3–5 h, the materials precipitated themselves from the reaction system after all the H_2O_2 was consumed up. Therefore, the material can be recovered easily by simply filtration or centrifugation. These materials show so high efficiency that the yields of GAC are as high as 91.3% and 94.4%, respectively (entries 1, 2 in Table 4). The other three materials (CPW11, CPW12 and TPW12) cannot dissolve in the reaction system. More interestingly, the activities of these three materials were very low (entries 3–5 in Table 4). These results demonstrate that the species of quaternary ammonium cations and POM anions all have great impact on their solubility and activities. It seems that only the ones with proper quaternary ammonium cations and POM anions can dissolve in the "H_2O_2-organic solvent" system and consequently can show very high activity in the selectively oxidative reaction with H_2O_2 as oxidant. The reaction temperature also has great impact on the catalytic efficiency of material CPW (entries 2, and 6–8 in Table 4). The highest GAC yield was obtained at 363 K. If the reaction temperature was low, the reaction rate was very low. However, if the temperature was too high, over-oxidation would occur and the yield of GAC was much lower, too. Thus a proper reaction temperature is very important. In addition, 30% and 15% H_2O_2 was also used as oxidant to investigate the effect of the H_2O_2 concentration (entries 9–12 in Table 4). High GAC yields were obtained when the high concentration H_2O_2 was used as the oxidant. For both CW and CPW material, the GAC yields decrease as the concentration of H_2O_2 decreases. But the yields of GAC decrease only a little and are still very high. All such results confirmed that the activities of these two reaction-controlled phase-transfer materials were significantly higher than the others. Then the material CPW was tried in the oxidation of various substrates to obtain dicarboxylic acids, including alicyclic-ketone, alicyclic-1,2-diol, linear terminal-diol and alicyclic-olefin. From entries 13–16 in Table 4, we can find that material CPW also shows high activity in the oxidation of different substrates. Except for cyclopentanone, these substrates can all be successfully oxidized to the corresponding dicarboxylic acids with high yield by H_2O_2 under the action of CPW. For cyclopentanone, the GAC yield was 64.3%, a bit

Table 4
Selective oxidation of CPDL as well as other substrates (olefin, 1,2-diol, ketone) to corresponding carboxyl acids on the phase-transfer materials[a]

Entry	Material[b]	Substrate	T (K)	$C_{H_2O_2}$ (wt.%)	Product	Yield[c] (%)	Efficiency of H_2O_2 (%)
1	CW	CPDL	363	50	GAC	91.3	83.0
2	CPW	CPDL	363	50	GAC	94.3	85.7
3	CPW11	CPDL	363	50	GAC	79.7	72.5
4	CPW12	CPDL	363	50	GAC	22.9	20.8
5	TPW12	CPDL	363	50	GAC	9.4	8.5
6	CPW	CPDL	353	50	GAC	87.3	79.4
7	CPW	CPDL	358	50	GAC	88.2	80.2
8	CPW	CPDL	368	50	GAC	93.9	85.4
9	CW	CPDL	363	30	GAC	90.4	82.2
10	CPW	CPDL	363	30	GAC	92.2	83.8
11	CW[d]	CPDL	363	15	GAC	88.4	80.4
12	CPW[d]	CPDL	363	15	GAC	90.6	82.4
13	CPW	Cyclopentanone	363	50	GAC	64.3	58.5
14	CPW	1,5-Pentanediol	363	50	GAC	77.6	70.5
15	CPW	CPE	358	50	GAC	83.1	75.5
16	CPW	Cyclohexene	358	50	Adipic acid	82.5	75.0
17	Re-CPW[e]	CPDL	363	50	GAC	64.2	58.4
18	Re-CW[f]	CPDL	363	50	GAC	62.8	78.6

[a] In all these reactions, the reaction conditions are: $n_{substrate}$:$n_{H_2O_2}$: $n_{cat.(W)}$ = 1:3.3:0.02; reaction time is 5 h (except for entries 11 and 12).

[b] The material CPW refers to $[\pi\text{-}C_5H_5NC_{16}H_{33}]_3\{PO_4[WO_3]_4\}$, CW refers to $[\pi\text{-}C_5H_5NC_{16}H_{33}]_2[W_2O_3(O_2)_4]$, CPW11 refers to $[\pi\text{-}C_5H_5NC_{16}H_{33}]_7[PW_{11}O_{39}]$, CPW12 refers to $[\pi\text{-}C_5H_5NC_{16}H_{33}]_3[PW_{12}O_{40}]$, TPW12 refers to $[C_{16}H_{33}N(CH_3)_3]_3[PW_{12}O_{40}]$, Re-CPW refers to the recovered CPW, and Re-CW refers to the recovered CW.

[c] The yield was based on the substrates.

[d] The reaction time is 8 h.

[e] The recovery of material CPW in this reaction was 64.2%.

[f] The recovery of material CPW in this reaction was 62.8%.

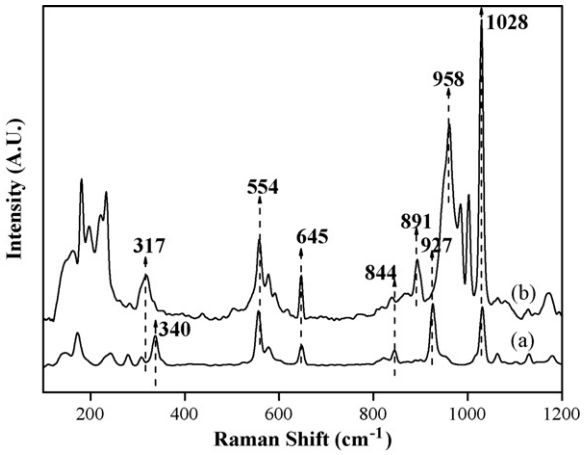

Fig. 4. Raman spectra of catalyst: (a) CW and (b) the recovered CW (Re-CW).

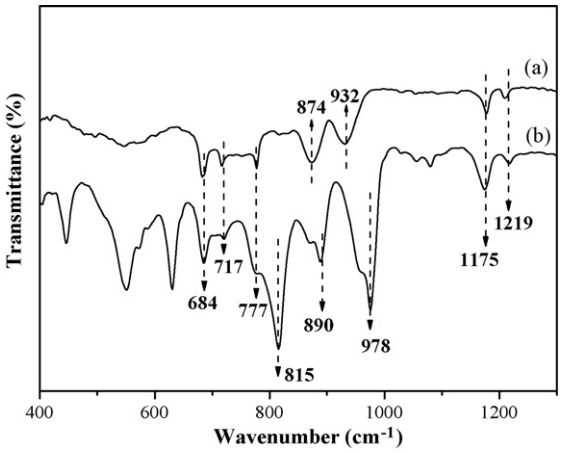

Fig. 5. FT-IR spectra of catalyst: (a) CW and (b) the recovered CW (Re-CW).

lower (entry 13 in Table 4) than the other substrates, suggesting that the oxidation of cyclopentanone is a little difficult since the reaction conditions are difficult to control. We also investigated the recovering and reusing behaviors of material CPW and CW (entries 17, 18 in Table 4). The activities of the recovered samples all decreased to 5–10% as compared to the fresh sample. However, the decrease of GAC yield for CW is very small (<5%). In addition, the recovery proportions of these two samples were as low as only about 65%. Thus we think that the intrinsic nature of the active sites changed definitely during the reaction and recovering process.

It is satisfactory to find that, for all these materials, the purity of the resulting GAC crystals is better than 99% (analyzed by GC) and the melting point is 369–370 K, similar to the literature value of 370–371 K. Hence, the resulting GAC product prepared in this process is also pure enough and can be used directly in most fields.

3.3.2. Characterization

3.3.2.1. Characterization of the fresh and the recovered CW. The fresh material CW and the recovered one Re-CW were all characterized by Raman spectroscopy, as shown in Fig. 4. In Fig. 4(a), CW shows Raman bands at 340, 554, 645, 844, 927 and 1028 cm^{-1}. The peaks at 340, 554, 844 and 927 cm^{-1} can easily be assigned to υ(W–O_2H), υ[W(O_2)] , υ(O–O) and υ(W=O), respectively [16,26]. They are all the characteristic peaks of $[W_2O_3(O_2)_4(H_2O)_2]_2-$ structure. It is easy to find that there is active oxygen in the structure, which may be the reason why this material is so active. The bands at 645 and 1028 cm^{-1} can be corresponded to the ammonium cation [8]. However, the Raman spectra of the recovered material Re-CW (see Fig. 4(b)) are very different from those of CW. The main Raman bands of Re-CW appear at 317, 554, 645, 891, 958 and 1028 cm^{-1}. The bands at 317, 554 and 958 cm^{-1} can be assigned to υ(W–O_2H), υ[W(O_2)] , and υ(W=O), respectively. Then we can find that the recovered material Re-CW also shows these three segments, but the position of the W–O_2H and W=O bands is a little different from that of CW, indicating that the structure of CW changes after the reaction so that the bond lengths in Re-CW are different from the corresponding ones in CW. In addition, no band of O–O bond appears in the Raman spectra of Re-CW, indicating the loss of active oxygen after the reaction for CW.

FT-IR spectra were also collected, as shown in Fig. 5. For the FT-IR spectra of the fresh CW sample (Fig. 5(a)), main bands at 684, 717, 777, 874, 932, 1175 and 1219 cm^{-1} appear. Those at 684, 717, 777, 1175 and 1219 cm^{-1} are attributed to the ammonium cation [8]. The band at 932 cm^{-1} can be attributed to the stretching mode of the W=O bond and that at 874 cm^{-1} to the mode of υ(W–O_b–W) (corner-sharing) [27–30]. In addition, no bands attributed to mode of υ(O–O) at 840 cm^{-1} are observed. However, there appears the band of υ(O–O) mode in the Raman spectra, suggesting that the symmetry of the local structure with O–O bond makes this band Raman active, but infrared inactive. The FT-IR spectra of the recovered material Re-CW (see Fig. 5(b)) is totally different from that of CW, identical to the result in the Raman experiments. Besides the bands at 684, 717, 777, 1175 and 1219 cm^{-1} that are due to the ammonium cation, characteristic bands at 978, 890, 815 cm^{-1} are also observed. The band at 932 cm^{-1} due to W=O vibration in the fresh CW material shifts to 978 cm^{-1} in the recovered material Re-CW. A similar result is also observed in the vibration region of υ(W–O_b–W), where the band shifts from 874 to 890 cm^{-1} [26,28,31]. The shifts indicate the changes of the bond lengths. In addition, a strong and broad band at 815 cm^{-1} appears, indicating the formation of a great number of W–O_c–W (edge-sharing) bonds [28–30]. This result suggests that the WO_x species polymerize after reaction by sharing the oxygen atoms in corner, which accords well with the Raman experiment results.

XPS investigations of binding energies and intensities of the surface elements provide information on the chemical states and relative quantities of the surface compounds. Peak-fitting results of W4f XPS spectra corresponding to fresh CW sample and to the recovered one are summarized in Fig. 6. Detailed binding energy values and quantitative results from the peak-fitting treatments of W4f are given in Table 5. From Table 5 and Fig. 6, an interesting phenomenon can be observed. A great amount of W^{5+} exists on the surface of the fresh CW sample. Similar phenomena can also be found in other tungsten-

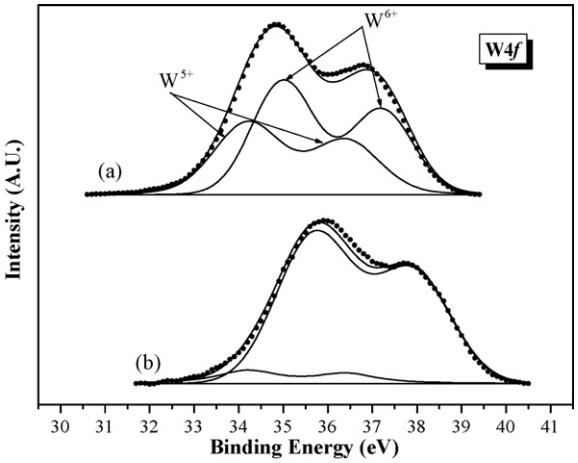

Fig. 6. XPS spectra of the W4f region for (a) fresh sample CW and (b) the recovered sample Re-CW.

containing materials [32]. In the preparation process of CW and CPW, the tungsten-containing compounds (such as Na_2WO_4 and tungstic acid) were complexed with H_2O_2, and all tungsten atoms should be in the highest value (+6). It is known that the $W(O_2)$ species is not very stable and will be decomposed by irradiation, thus leading the appearance of W^{5+} on the surface of the material. The percentage of W^{5+} in CW sample is very high (41.7%) and the ease to be reduced also indicates that the structure of this sample was not very stable. After the reaction, the amount of W^{5+} in the material decreased abruptly; only 8.6% W^{5+} was detected, indicating that the structure of the recovered material Re-CW is more stable than the corresponding fresh one. After the reaction the binding energy of W^{6+} also changes (see Table 5). The binding energy of $W4f_{7/2}$ shifts from 37.2 for CW to 37.8 eV for Re-CW. The phenomenon that the binding energy of W4f shifts towards higher binding energy implies that the coordination circumstance of the W^{6+} ion changes obviously after the material was recovered.

3.3.2.2. Characterization of the fresh and the recovered CPW. The fresh and the recovered CPW sample under

Table 5
Chemical state of surface tungsten in different materials detected by XPS

Sample	Binding energy for W4f/eV				W^{6+}/W^{5+a}
	$W^{6+}4f_{5/2}$	$W^{6+}4f_{7/2}$	$W^{5+}4f_{5/2}$	$W^{5+}4f_{7/2}$	
CW	37.2	35.1	36.4	34.2	1.4
Re-CW	37.8	35.7	36.4	34.2	10.6
CPW	37.4	35.2	36.4	34.2	0.65
Re-CPW-1[b]	37.8	35.6	37.0	34.8	4.21
Re-CPW-2[c]	38.0	35.8	–	–	–
Re-CPW-3[d]	38.2	36.0	36.4	34.2	11.4

[a] Calculated according to the curve-fitting results of the W4f XP spectra of various materials.
[b] Re-CPW-1 is the recovered material of CPW after the reaction was carried out at 353 K for 5 h.
[c] Re-CPW-2 is the recovered material of CPW after the reaction was carried out at 363 K for 5 h.
[d] Re-CPW-3 is the recovered material of CPW for the second run after the reaction was carried out at 353 K for 5 h.

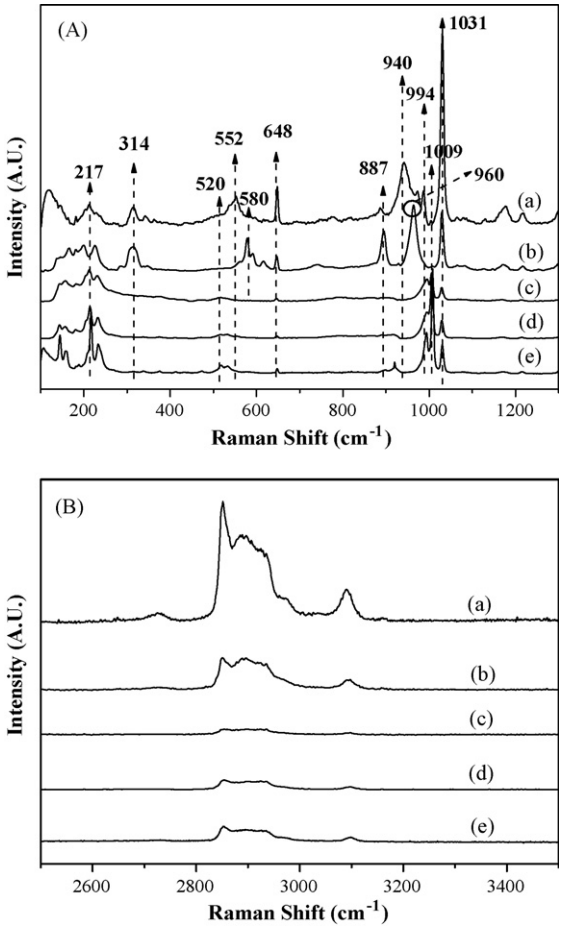

Fig. 7. Raman spectra of: (a) fresh material CPW; (b) the recovered material of CPW after the reaction was carried out at 353 K for 5 h; (c) the recovered material of CPW after the reaction was carried out at 363 K for 5 h; (d) the recovered material of CPW for the second run after the reaction was carried out at 353 K for 5 h. The range of Raman shift of figure (A) is 100–1300 cm^{-1} and that of (B) is 1250–3500 cm^{-1}.

different reaction conditions were all characterized by Raman spectroscopy, as shown in Fig. 7. In order to give a better assignment of the Raman bands of the materials, we also measured material CPW12 with the Keggin structure $PW_{12}O_{40}^{3-}$ anion under the same conditions. As seen in Fig. 7(A(a)), CPW shows Raman bands at 314, 552, 648, 887, 940 and 1031 cm^{-1}. Those peaks at 314, 552, and 940 cm^{-1} can easily be assigned to υ(W–O_2H), υ[W(O_2)], υ(W=O), respectively [16,26], indicating that there is active oxygen in the structure of the fresh CPW sample, which may be one of the reasons for the ultra high activity of the reaction-controlled phase-transfer material. The weak band at 887 cm^{-1} is due to the presence of excess free hydrogen peroxide [16], which may have been entrapped during the preparation process. The bands at 648 and 1031 cm^{-1} correspond to the ammonium cation [8]. When this material was recovered after the reaction was carried out at 353 K for 5 h, some changes appeared in its Raman spectra (see Fig. 7(A(b))). The band at 552 cm^{-1} due to W(O_2) vibration in the fresh CPW sample shifts to 580 cm^{-1} in the recovered one. A similar result was also observed in the vibration region of υ(W=O), where the band shifts from 940 to

960 cm^{-1}. As mentioned above, the shifts indicate the changes of the bond lengths, thus suggesting that the structure of CPW sample changed after the reaction. When the fresh sample was recovered after the reaction was carried out at higher temperature (363 K) for 5 h or was recovered for the second time, the corresponding Raman spectra changed dramatically (see Fig. 7(A(b) and (c))). The intensity of the 1031 cm^{-1} band decreases greatly, while the 648 cm^{-1} band almost disappears, indicating that the content of ammonium cation in the recovered material is much lower after the reaction. In addition, the bands at 314, 887 and 940 cm^{-1} also disappear, indicating the absence of W–O_2H, free H_2O_2 and W=O. The band at 552 cm^{-1} shifts to 520 cm^{-1}, indicating the structure change of W(O_2). New bands at 217, 234, 994 and 1009 cm^{-1} appear, which are similar to those of spectra (e)——[π-$C_5H_5NC_{16}H_{33}]_3[PW_{12}O_{40}]$ (CPW12). Interestingly, spectra (c), (d) and (e) show nearly the same Raman spectra, which have the same main bands at 217, 234, 520, 994 and 1009 cm^{-1}. The very strong band at 1009 cm^{-1} is the characteristic of phosphotungstate with Keggin structure, which is attributed to υ_s(W=O_t) (O_t = terminal oxygen); the strong bands at 994 cm^{-1} are assigned to υ_{as}(W=O_t); and the band at 217 cm^{-1} can be attributed to υ_s(W–O_μ) (O_μ = oxygen in bridge or μ-oxo) [31]. The presence of bridging oxygen indicates the presence of polymerization of WO_x species (one tungsten atom is linked to the other by bridging oxygen). All the changes of Raman spectra suggest that the recovered material does not keep the initial structure of the fresh one, but polymerizes to a Keggin structure with bridging O_μ. We also noticed that if the reaction temperature was not so high and the material was recovered just for the first time, the structure will not change totally (see spectra (b)); but if the reaction temperature was high or the material was recovered for more than one time, the structure will change completely to Keggin structure. The result indicates that the structure change for CPW sample was a gradual process.

In the 1250–3500 cm^{-1} range of Raman spectra, only bands of ammonium cation are observed [8]. If one compares spectra (b) with (a) in Fig. 7(B), the intensity of all Raman bands are decreased, indicating that the content of ammonium cation in the recovered material is lowered. The intensity of Raman bands in spectra (c) and (d) decreases seriously, and the intensity of the bands in spectra (c), (d) and (e) is nearly the same, suggesting that they have similar ammonium cation contents. We can also observe the same tendency that the structure change for CPW material was a gradual process.

FT-IR spectra were also collected, as shown in Fig. 8. For the FT-IR spectra of the fresh CPW sample (Fig. 8(a)), main bands at 886, 945 and 1097 cm^{-1} appear, along with the bands of ammonium cation at 680, 715, 776, 1173 and 1209 cm^{-1}. The broad bands at 1079 and 935 cm^{-1} can be ascribed to the stretching mode of the P–O bond and the W=O bond, respectively [27]. Based on the results of the literature [28–30], the IR band at 886 cm^{-1} can be attributed to the mode of υ(W–O_b–W) (corner-sharing). However, no band at 815 cm^{-1} (attributed to υ(W–O_c–W) (edge-sharing)) is observed, indicating the absence of polymerization of WO_x species.

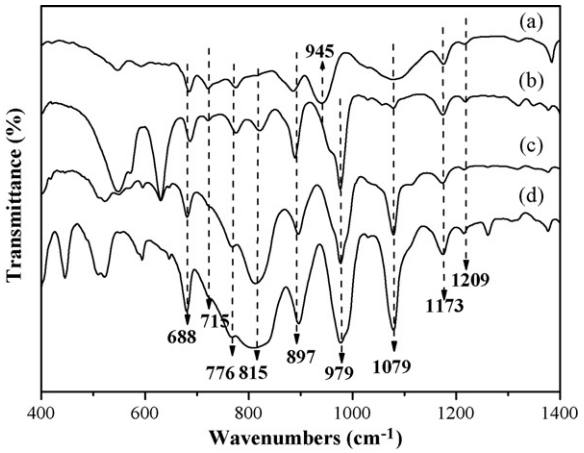

Fig. 8. FT-IR spectra of: (a) fresh material CPW; (b) the recovered material of CPW after the reaction was carried out at 353 K for 5 h; (c) the recovered material of CPW after the reaction was carried out at 363 K for 5 h; (d) the recovered material of CPW for the second run after the reaction was carried out at 353 K for 5 h.

The FT-IR spectra of the sample recovered after the reaction was taken at 353 K for 5 h is a little different (see Fig. 8(b)). Firstly, the band at 945 cm^{-1} due to W=O vibration in the fresh CPW material shifts to 979 cm^{-1} in the recovered sample. Secondly, an additional small band appears at 815 cm^{-1}, which is due to W–O_c–W bond, implying that some WO_x species polymerized after reaction. If the reaction temperature was higher (363 K) or the material was recovered more than once, the band at 815 cm^{-1} in the spectra became very large, indicating that a great number of W–O_c–W bonds have been formed. These results accord well with those from the Raman spectra.

In order to clearly investigate the structure change of CPW after the reaction, we also carried out ^{31}P MAS NMR tests, as shown in Fig. 9. The spectrum of the fresh sample (Fig. 9(a)) shows a broad peak from 10 to −20 ppm, which can be assigned

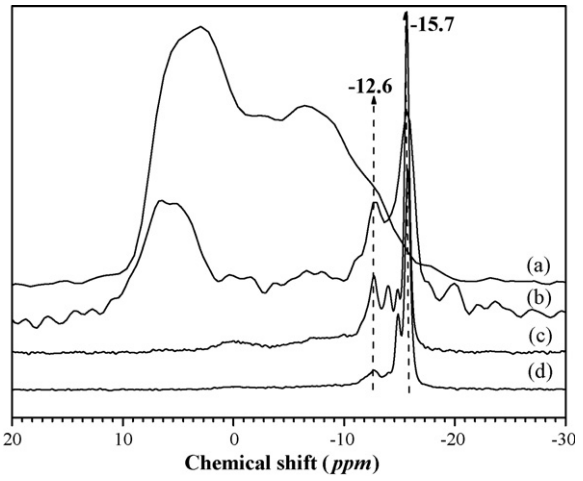

Fig. 9. ^{31}P MAS NMR spectra of material: (a) fresh material CPW; (b) the recovered material of CPW after the reaction was carried out at 353 K for 5 h; (c) the recovered material of CPW after the reaction was carried out at 363 K for 5 h; (d) the recovered material of CPW for the second run after the reaction was carried out at 353 K for 5 h.

to heteropoly tungstophosphates with the ratio of P/W from 1/2 to 1/12 [33]. Thus we can get the same conclusion as reported previously [8,11] that CPW is not a pure compound as shown in the molecular formula with the P/W ratio of 1/4, but a mixture that consists of several compounds with different P/W ratios. When the material was recovered after the reaction was taken at 363 K for 5 h, the ^{31}P NMR spectra changes (see Fig. 9(b)). Three main peaks are observed in the spectra (b). The broad peak from 10 to 0 ppm is also assigned to heteropoly tungstophosphates with different P/W ratios. The position and shape of this peak is similar to the one of fresh CPW, but the intensity is lower. Two additional sharp peaks appear at −12.6 and −15.7 ppm, which are all characteristic peaks of compounds with Keggin structure [29,30] and can be attributed to $(PW_{11}O_{39})^{7-}$ and $(PW_{12}O_{40})^{3-}$, respectively [34], illustrating that, after reaction under this condition, some structure of the fresh material was preserved, but some changes to the Keggin structure occur. If the reaction temperature was higher (363 K) or the material was recovered more than once, the spectra changes totally (see Fig. 9(c) and (d)). Only two main peaks at −12.6 and −15.7 ppm can be observed, and the peak at −12.6 ppm becomes smaller, suggesting that, after reaction under these conditions, the material mainly changes to $[\pi\text{-}C_5H_5NC_{16}H_{33}]_3\ [PW_{12}O_{40}]$ with a small amount to $[\pi\text{-}C_5H_5NC_{16}H_{33}]_7[PW_{11}O_{39}]$. So we can also observe the "gradual process" of the material structure changes, which accords well with the Raman and FT-IR results. The ^{31}P MAS NMR spectra reveals more clearly that, after reaction, the PO_4^{3-} and WO_x species polymerized to form more stable $(PW_{12}O_{40})^{3-}$ and $(PW_{11}O_{39})^{7-}$(small amount) with Keggin structure. Considering the activity results that the catalytic performance of $[\pi\text{-}C_5H_5NC_{16}H_{33}]_3\ [PW_{12}O_{40}]$ and $[\pi\text{-}C_5H_5NC_{16}H_{33}]_7[PW_{11}O_{39}]$ are low (see entries 3 and 4 in Table 4, respectively), especially for $[\pi\text{-}C_5H_5NC_{16}H_{33}]_3\ [PW_{12}O_{40}]$, we can get the reason why the activity of the recovered Re-CPW sample is low (see entry 17 in Table 4).

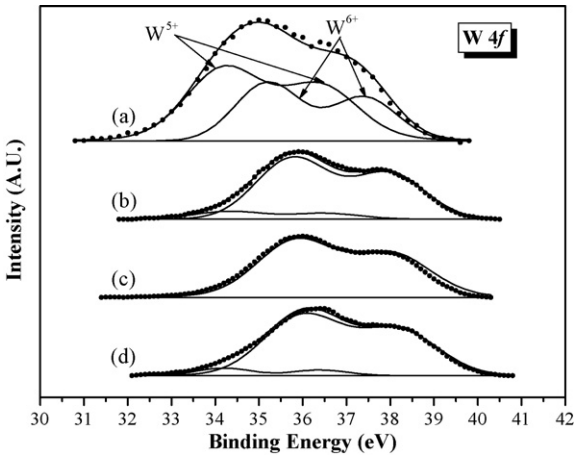

Fig. 10. XPS spectra of the W4f region for: (a) fresh material CPW; (b) the recovered material of CPW after the reaction was carried out at 353 K for 5 h; (c) the recovered material of CPW after the reaction was carried out at 363 K for 5 h; (d) the recovered material of CPW for the second time after the reaction was carried out at 353 K for 5 h.

Peak-fitting results of W4f XPS spectra corresponding to fresh CPW sample and its recovered ones are summarized in Fig. 10. Detailed binding energy values and quantitative results from the peak-fitting of W4f are given in Table 5. From Table 5 and Fig. 10, we can find similar changing tendencies as compared with the information of CW sample. There is also a great part of W^{5+} in the fresh CPW sample. The quantity of W^{5+} decreases in the recovered material, and the more times the material was recovered, the less W^{5+} was left (the W^{5+}% in Re-CPW-1 is 19.2% and in Re-CPW-3 is 8.1%, respectively). Even in the Re-CPW-2 sample that was recovered after the reaction was carried out at 363 K for 5 h, nearly no W^{5+} was detected. As mentioned above, these results indicate that, after the reaction, a more stable material structure formed. The binding energies of W4f all shift towards higher energy for the recovered materials, indicating that the structure of the recovered material changed, too. All these results are in line with those from the Raman, FT-IR and ^{31}P MAS NMR.

4. Conclusions

Oxidation of CPDL to GAC was carried out on three main kinds of materials. The homogeneous tungstic acid catalyst shows very high GAC yield (91.2%). The heterogeneous tungsten-containing MCM-41 catalyst synthesized by in situ method shows high WO_3 species dispersion as compared to the one synthesized by the wet-impregnation method. The GAC yield is 70.5% over the 20% W-doped-MCM-41 catalyst. The phase-transfer materials ($[\pi\text{-}C_5H_5NC_{16}H_{33}]_2[W_2O_3(O_2)_4]$ (CW) and $[\pi\text{-}C_5H_5NC_{16}H_{33}]_3\ \{PO_4[WO_3]_4\}$(CPW)) showed very high activity and the GAC yield can reach 91.3% and 94.3%, respectively. The unique characteristic that the material dissolved completely in the reaction solution during the reaction but precipitated itself after the reaction made them possess the advantages of both homogeneous and heterogeneous catalysis, which can be recovered conveniently by centrifugation or filtration. The GAC yield decreased a little over the recovered Re-CW sample, and decreased much on Re-CPW sample. Raman, FT-IR and ^{31}P MAS NMR spectra revealed that the structure of the phase-transfer material changed after the reaction. After the reaction the WO_x species in both CW and CPW polymerize by forming W–O_c–W bond, and the structure of CPW changes gradually to more stable Keggin structure as $[\pi\text{-}C_5H_5NC_{16}H_{33}]_3[PW_{12}O_{40}]$ and $[\pi\text{-}C_5H_5NC_{16}H_{33}]_7[PW_{11}O_{39}]$ (just a small amount). XPS results showed that the chemical state of tungsten in the recovered materials of CW and CPW all changed obviously after the reaction. The amount of W^{5+} in the fresh materials is very high, but much lower in the recovered materials. The binding energies also shift towards higher energy for the recovered materials, suggesting the coordination circumstances change of the materials from before to after reaction. Developing new materials with more excellent activity and stability as well as anti-leaching character is the key role for the further large-scale application in industry of this new green process and those studies are under way.

Acknowledgements

This work was financially supported by the Major State Basic Resource Development Program (Grant No. 2003CB615807), NSFC (Project 20407006, 20573024), and the Natural Science Foundation of Shanghai Science & Technology Committee (06JC14004).

References

[1] M. Besson, F. Gauthard, B. Horvath, P. Gallezot, J. Phys. Chem. B 109 (2005) 2461–2467.
[2] R.W. Johnson, C.M. Pollock, R.R. Cantrell, in: J. Krodchwitz (Ed.), 4th ed., Kirk-Othmer Encyclopedia of Chemical Technology, vol. 8, J. Wiley & Sons, New York, 1993.
[3] A.K. Sureh, M.M. Sharma, T. Sridhar, Ind. Eng. Chem. Res. 39 (2000) 3958–3997.
[4] A. Castellan, J.C.J. Bart, S. Cavallarro, Catal. Today 9 (1991) 237–254, 255–283, 285–299.
[5] K. Sato, M. Aoki, R. Noyori, Science 281 (1998) 1646–1647.
[6] R. Noyori, M. Aoki, K. Sato, Chem. Commun. (2003) 1977–1986.
[7] H. Chen, W. Dai, X. Yang, R. Gao, Y. Cao, K. Fan, Petrochem. Technol. 35 (2006) 119–123 (in Chinese).
[8] H. Chen, W. Dai, X. Yang, R. Gao, Y. Cao, K. Fan, Appl. Catal. A: Gen. 309 (2006) 62–69.
[9] H. Chen, W. Dai, J. Deng, K. Fan, Catal. Lett. 81 (2002) 131–136.
[10] X. Yang, W. Dai, H. Chen, Y. Cao, H. Li, H. He, K. Fan, J. Catal. 229 (2005) 259–263.
[11] J. Gao, Y. Chen, B. Han, Z. Feng, C. Li, N. Zhou, S. Gao, Z. Xi, J. Mol. Catal. A: Chem. 210 (2004) 197–204.
[12] Y. Sun, Z. Xi, G. Gao, J. Mol. Catal. A: Chem. 166 (2001) 219–224.
[13] J.A. Bailey, P.W. Griffith, C.B. Parkin, J. Chem. Soc., Dalton Trans. 11 (1995) 1833–1837.
[14] C. Brevard, R. Schimpf, G. Tourne, C.M. Tournet, J. Am. Chem. Soc. 105 (1983) 7059–7063.
[15] X. Yang, W. Dai, H. Chen, J. Xu, H. Li, Y. Cao, K. Fan, Appl. Catal. A: Gen. 283 (2005) 1–8.
[16] C. Aubry, G. Chottard, N. Platzer, J.M. Brégeault, R. Thouvenot, F. Chaureau, C. Huet, H. Ledon, Inorg. Chem. 30 (1991) 4409–4415.
[17] L. Sales, C. Aubry, R. Thouvenot, F. Robert, C.D. Morin, G. Chottard, H. Ledon, Y. Jeannin, J.M. Brégeault, Inorg. Chem. 33 (1994) 871–878.
[18] D.C. Duncan, R.C. Chambers, E. Hecht, C.L. Hill, J. Am. Chem. Soc. 117 (1995) 681–691.
[19] L. Salles, J.Y. Piquemal, R. Thouvenot, C. Minot, J.M. Brégeault, J. Mol. Catal. A: Chem. 117 (1997) 375–387.
[20] N.M. Grecley, W.P. Griffith, A.C. Laemmel, H.S. Nogueira, B.C. Parkin, J. Mol. Catal. A: Chem. 117 (1997) 185–198.
[21] H. Zeng, G.R. Newkome, C.L. Hill, Angew. Chem. Int. Ed. 39 (2000) 1771–1774.
[22] L. Plault, A. Hauseler, S. Nlate, D. Astruc, J. Ruiz, S. Catard, R. Neumann, Angew. Chem. Int. Ed. 43 (2004) 2924–2928.
[23] S. Nalte, D. Astruc, R. Neumann, Adv. Synth. Catal. 346 (2004) 1445–1448.
[24] C. Venturello, M. Ricci, J. Org. Chem. 51 (1986) 1599–1602.
[25] Z. Xi, N. Zhou, Y. Sun, K. Li, Science 292 (2001) 1139–1141.
[26] N.J. Campbell, A.C. Dengel, C.J. Edwards, W.P. Griffith, J. Chem. Soc., Dalton Trans. 6 (1989) 1203–1208.
[27] C. Venturello, R. D'Aloisio, J. Org. Chem. 53 (1988) 1553–1557.
[28] E. Radkov, R.H. Beer, Polyhedron 14 (1995) 2139–2143.
[29] N.I. Kuznetsova, L.G. Detusheva, L.I. Kuznetsova, M.A. Fedotov, V.A. Likholobov, J. Mol. Catal. A: Chem. 114 (1996) 131–139.
[30] L.R. Pizzio, C.V. Cáceres, M.N. Blanco, Appl. Surf. Sci. 151 (1999) 91–101.
[31] C. R'Deltcheff, M. Fournier, R. Franck, R. Thouvenot, Inorg. Chem. 22 (1983) 207–216.
[32] X. Yang, W. Dai, C. Guo, H. Chen, Y. Cao, H. Li, H. He, K. Fan, J. Catal. 234 (2005) 438–450.
[33] M.T. Pope, Heteropoly and Isopoly Oxometalates, vol. 66, Springer-Verlag, Berlin, 1983.
[34] Y. Chen, J. Zhang, X. Liu, J. Gao, X. Han, X. Bao, N. Zhou, S. Gao, Z. Xi, Catal. Lett. 93 (2004) 41–46.